RSC Advances

PAPER

View Article Online
View Journal | View Issue

Cite this: *RSC Adv.*, 2024, **14**, 25289

Fabrication and characterization of TPGS-modified chlorogenic acid liposomes and its bioavailability in rats†

Jian-jun Zhang,[a] Qiu-shui Luo,[a] Qing-qing Li,[a] Qian Xu,[a] Xiang Geng *[a] and Jian-hua Xiong*[ab]

Chlorogenic acid (CGA), a polyphenol compound, exhibits excellent anti-oxidative, anti-hypoxic, antibacterial, antiviral, and anti-inflammatory activities, however the bioactivity of it has not been fully utilized *in vivo* due to its instability and low bioavailability. To address these issues, we prepared and characterized CGA-TPGS-LP, which is a TPGS-modified liposome loaded with CGA. The pharmacokinetics of CGA-TPGS-LP were studied in rats after oral administration. CGA-TPGS-LP was fabricated using a combination of thin film dispersion and ion-driven methods. The liposomes were observed to be uniformly small and spherical in shape. Their membranes were composed of lecithin, cholesterol, and TPGS lipophilic head with a TPGS hydrophilic tail chain coating on its surface. The loading efficiency and encapsulation efficiency were found to be 11.21% and 83.22%, respectively. The physicochemical characterisation demonstrated that the CGA was present in an amorphous form and retained its original structural state within the liposomal formulation. The stability of CGA was significantly improved by fabricating TPGS-LP. CGA-TPGS-LP exhibited good sustained-release properties in both simulated gastric and intestinal fluids. Following oral administration, ten metabolites were identified in rat plasma using UPLC-QTOF-MS. UPLC-QqQ-MS/MS quantitative analysis demonstrated that the oral bioavailability of CGA encapsulated in TPGS-modified liposomes was enhanced by 1.52 times. In addition, the three main metabolites of CGA had higher plasma concentrations and slower degradation rate. These results demonstrate that TPGS-modified liposomes could be a feasible strategy to further enhance the oral bioavailability of CGA, facilitating its clinical use.

Received 5th June 2024
Accepted 26th July 2024

DOI: 10.1039/d4ra04116j

rsc.li/rsc-advances

1. Introduction

Chlorogenic acid (CGA), known as 3-caffeoylquinic acid, is a polyphenol that is widely distributed in higher plants.[1] The substance has various benefits, including antioxidant, antiviral, antitumor, antibacterial, anti-inflammatory properties, and the ability to improve cardiovascular health and modulate plasma fat concentration.[2–4] When added to the feed at a rate of 400 mg kg^{-1}, CGA can enhance the growth performance, immune function, and antioxidant capacity of common carp. It can also improve the health of the intestine and liver through Keap-1/Nrf2 and NF-κB signaling pathways.[5] Furthermore, CGA exhibited a protective effect against aflatoxin B1-induced hepatic damage by regulating redox status and inflammation.[6] In addition, a previous study indicated that CGA extracted from *Lonicera japonica* leaves had a stronger antibacterial effect against Gram-positive bacteria *Staphylococcus aureus* and Gram-negative bacteria *Escherichia coli* than the two most commonly used food preservatives, potassium sorbate and sodium benzoate.[3] CGA has potential for use in health foods and pharmaceuticals due to its positive effects. However, its tachy-metabolism, instability, and poor oral absorption efficiency result in poor bioavailability in rats, hindering practical application. Therefore, a formulation is necessary to provide protective effects during processing and storage and delay rapid clearance of CGA after oral administration. Constructing a delivery vehicle is deemed an efficient method to shield it from detrimental environmental factors and improve oral bioavailability.

Liposome formulations are considered a safe and effective approach to improving drug delivery properties.[7] The main body of liposomes consists of phosphatidyl-choline, which has a structure similar to that of biological membranes. Therefore, liposomes have good biocompatibility and lower cytotoxicity.[8] They are versatile drug carriers with a hydrophilic core and phospholipid bilayer membranes shell that can accommodate both hydrophilic and hydrophobic drugs.[9] Studies have shown

[a]*College of Food Science and Engineer, Jiangxi Agricultural University, Nanchang 330045, China. E-mail: 396802874@qq.com; 809472384@qq.com*

[b]*Key Lab for Agricultural Product Processing and Quality Control of Nanchang City, Nanchang 330045, China*

† Electronic supplementary information (ESI) available. See DOI: https://doi.org/10.1039/d4ra04116j

that liposomes can improve the bioavailability and stability of encapsulated compounds.[10] However, liposomes are prone to aggregation, fusion, or degradation during storage due to their soft material attributes.[11] Interactions between liposomal particles and external environmental factors can cause morphological and structural changes, leading to nutrient leakage. These limitations restrict their widespread use. To stabilize liposomal particles, modifying the liposomal membrane has been proposed.

TPGS is a water-soluble excipient synthesized by esterifying vitamin E succinate with polyethylene glycol 1000. It is considered safe for human consumption by the US Food and Drug Administration (FDA).[12] TPGS has excellent surfactant properties due to its combination of the lipophilic group of vitamin E and the hydrophilic long chain of polyethylene glycol. Consequently, it is employed extensively as a solubilizer, penetration enhancer, emulsifier, stabilizer, and absorption promoter.[13–15] In addition, numerous delivery systems based on modified TPGS have been developed for the administration of active molecules and drugs with improved bioavailability and drug efficacy. Research by Farooq *et al.*[16] shows that the use of TPGS-coated liposomes can enhance the cytotoxicity and cellular uptake of vorinostat in breast cancer cells. Examples of such compounds include docetaxel,[17] and brinzolamide.[18]

Currently, no studies have been found that utilise TPGS-modified liposomes as a delivery vehicle to enhance the bioavailability of CGA. Therefore, we fabricated CGA-TPGS-LP using a combination of the thin film dispersion method and the ion-driven method. We detected the polydispersity index (PDI), particle size, entrapment efficiency (EE), and zeta potential of CGA-TPGS-LP. The liposomal formulations underwent examination using Fourier transform infrared spectroscopy, transmission electron microscopy, and differential scanning calorimetry. The study estimated their storage stability and *in vitro* cumulative release characteristics in both simulated intestinal fluid and simulated gastric fluid. Additionally, their oral bioavailability was studied in a rat trial. UPLC-QTOF-MS was used to qualitatively identify the metabolites of CGA in rat plasma, while UPLC-QqQ-MS/MS was used to quantitatively determine the oral availability of CGA after administration.

2. Materials and methods

2.1. Chemicals

CGA (>95%) was isolated and purified from Honeysuckle suspension cells obtained through induction culture in our laboratory.[19] It was later identified by comparing its mass spectrometry (MS) and high-performance liquid chromatography (HPLC) values with those of the CGA control standards. The CGA and Rutin standards were obtained from Merck Co., Ltd (Darmstadt, Germany). Soy phosphatidylcholine (SPC), which consists mainly of phosphatidylcholine (90%), was supplied by Shanghai Yuanye Bio-Technology Co., Ltd (Shanghai, China). D-α-Tocopheryl polyethylene glycol 1000 succinate (TPGS) and cholesterol (Chol) were provided by Aladdin Industrial Corporation (Shanghai, China). Calcium acetate monohydrate and sodium sulfate were supplied by Xilong Scientific (Shanghai, China). Pepsin (1 : 10 000) and pancreatin (1 : 125) were provided by Beijing Solarbio Science & Technology Co., Ltd (Beijing, China). All other reagents used in this experiment are analytically pure.

2.2. Animals

The male Sprague-Dawley rats were purchased from Hunan Slack Jing Da Laboratory Animal Co., Ltd in Changsha City, Hunan province, China. They were kept in a experimental room with a 12/12 h light/dark cycle at a temperature of 23–25 °C and had ad libitum access to food and water. All follow-up experiments were conducted in accordance with the experimental guidelines and animal management protocols of Jiangxi Agricultural University.

2.3. Fabrication of CGA-LP and CGA-TPGS-LP

The CGA-LP and CGA-TPGS-LP liposomes were prepared using the thin film dispersion method combined with the ion-driven method.

Formation steps of blank liposomes: In brief, SPC, Chol, and TPGS (only in the TPGS-retouched liposomes) were dissolved in 10 mL of ethanol at 50 °C. The ethanol was then evaporated using a rotary evaporator at 40 °C until a thin dried film formed. Subsequently, the thin film was hydrated with 10 mL of 0.12 mol per L calcium acetate aqueous solution for 30 min. The blank liposomes were collected after using probe ultrasonication for 10 min (Power 380 W, 3 s burst, 3 s pause) in an ice bath.

Ion-driven drug loading: The blank liposomes were transferred to a dialysis bag and placed in 0.12 mol per L sodium sulfate solution overnight to remove calcium acetate from the outside of the liposomes. Subsequently, the blank liposomes were mixed with 10 mL of CGA aqueous solution and incubated for 1.5 h at 40 °C under quick magnetic stirring. CGA was loaded into the liposomes through ion drive. The resulting nanoparticles were collected as either CGA-LP or CGA-TPGS-LP suspension after passing through a 0.22 μm filter to remove bacteria. A portion of liposome suspension was mixed with sucrose, which acted as a lyoprotectant at a final concentration of 12%. The resulting mixture was then used to create a lyophilized powder using a vacuum freeze dryer from Millrock Technology in Germany.

The list of different materials is presented as an $L_9(3^4)$ orthogonal matrix experiment in Table 1. The evaluation criterion used to screen the optimal formulations was EE.

Table 1 Orthogonal test design: $L_9(3^4)$ of CGA-TPGS-LP liposomes

	Factor			
	A	B	C	D
Level	SPC (mg)	SPC/CGA (w/w)	SPC/Chol (w/w)	SPC/TPGS
1	350	3 : 1	5 : 1	6 : 1
2	400	4 : 1	7 : 1	8 : 1
3	450	5 : 1	9 : 1	10 : 1

2.4. Analysis of encapsulation efficiency (EE) and loading efficiency (LE)

The EE and LE were analyzed through HPLC method. Firstly, aliquots (100 μL) of newly prepared liposome suspension were directly centrifuged at 10 000 rpm for 30 min at 4 °C. The collected supernatant was diluted 10 times and kept as free CGA sample. Simultaneously, several other aliquots (100 μL) of the liposome suspension were mixed with isopropanol (900 μL) to disrupt the structure of the liposomes and release free and entrapped CGA. After being diluted and filtered through a 0.22 μm organic filter membrane, the solution was injected into the HPLC.

The CGA content in solution was detected using the Waters e2695 HPLC system (Waters Corp., Milford, MA, USA) equipped with a 2998 PDA detector. Chromatographic separation was performed at 25 °C using a Symmetry C18 column (5 μm, 4.6 × 250 mm; Waters Technologies Inc., USA) with a mobile phase comprising 25% acetonitrile and 75% aqueous phase (containing 0.2% acetic acid). The flow rate was 1 mL min^{-1}, the injection volume was 20 μL, and the measured wavelength was 327 nm. The LE and EE were calculated using the following equations:

$$EE = \frac{\text{total amount of drug} - \text{free amount of drug}}{\text{total amount of drug}} \times 100\%$$

$$LE = \frac{\text{weight of drug loaded in liposomes}}{\text{total amount of ingredients in formulation}} \times 100\%$$

2.5. Characterization of blank liposome, CGA-LP and CGA-TPGS-LP

2.5.1. Measurements of liposomes size and zeta potential. The particle size, polydispersity index (PDI), and zeta potential of the samples were measured using a Zetasizer Nano ZS (Malvern Instruments Ltd, UK) at room temperature. Prior to measurement, the liposome suspension samples were diluted 100-fold with ultrapure water. Each sample was measured three times.

2.5.2. Transmission electron microscopy (TEM) photography. The liposomes' morphology and shape were determined using a Tecnai G2 Spirit transmission electron microscope (FEI, USA) operating at a voltage of 120 kV.

The liposome suspension was diluted 100-fold in ultrapure water and dropped onto a copper grid coated with a carbon membrane. After the samples naturally dried, 2% phosphotungstic acid was added to stain them for 5 min, and any excess liquid was removed with filter paper. The samples were then observed.

2.5.3. Fourier transform infrared (FTIR) analysis. The lyophilized liposome powder was mixed with pre-dried KBr powder and ground into a fine powder. The ground sample was compressed into pellets. The infrared spectra of the pellets were then detected using a Nicolet 5700 FTIR spectrometer (Nicolet, Madison, WI, USA).

2.5.4. Differential scanning calorimetry (DSC) analysis. Approximately 5 mg of liposome lyophilized powder was placed in a standard aluminum crucible and then sealed. The control was an empty, sealed aluminum crucible. DSC analysis was performed using a NETZSCH DSC 214 Polyma instrument (Netzsch, Germany) with a heating rate of 10 °C min^{-1}. The samples were heated from 50 to 300 °C with a flow of nitrogen gas.

2.5.5. Release study in SGF and SIF. Simulated intestinal fluid (SIF) and simulated gastric fluid (SGF) were prepared according to the parameters outlined in the United States Pharmacopeia.[20] The *in vitro* release of CGA-TPGS-LP and free CGA was investigated using a dialysis bag under sink conditions. The experiment involved dispersing 1 mL of CGA and liposome suspension in 9 mL of SGF/SIF (with enzyme) with a CGA concentration of 0.4 mg mL^{-1}. The resulting mixture was then transferred into a dialysis bag with a molecular cutoff of 8 kDa, which had been activated by boiling for 15 min in a mixture (pH 8.0) containing 2% (W/V) sodium bicarbonate and 1 mmol per L EDTA, and washing thoroughly. The bag was then sealed and placed into a beaker containing 1000 mL of SGF/SIF without the enzyme. The system was maintained at a temperature of 37 ± 0.5 °C and continuously agitated using magnetic stirring. The dialysis exudate was collected at predetermined time points (0.167, 0.5, 1, 1.5, 2, 2.5, 3, 4, 5, 6, 8, and 12 h) and filtered through a 0.22 μm hydrophilic filter membrane after centrifugation at 10 000 rpm for 10 minutes. An equal volume of fresh release media was added to the beaker after each collection. The concentration of CGA in the filtered solution was analyzed using HPLC.

2.5.6. Stability of CGA in CGA-TPGS-LP and CGA-LP. The storage stability of CGA-LP and CGA-TPGS-LP liposomal formulation was evaluated over a period of 30 days. The liposome suspension was stored at 4 °C and natural lighting, and the encapsulation efficiency was measured on days 1, 5, 10, 15, 20, 25, and 30.

2.6. Pharmacokinetic studies in rats

After a one-week adaptation period, twelve rats were randomly divided into two groups: CGA and CGA-TPGS-LP. All rats were fasted overnight and allowed to drink water freely before the pharmacokinetic study. The two groups of rats were administered 3 mL of either CGA solution or CGA-TPGS-LP suspension *via* intragastric administration, with a CGA dose of 40 mg kg^{-1} bwt. Blood samples of 200 μL were collected from the tail vein at predetermined times (0.083, 0.167, 0.5, 1, 2, 3, 4, 6, and 8 h) after oral administration into K2-EDTA anticoagulant tubes. Food and water were replenished 2 h after oral administration. Plasma samples were obtained by centrifuging the blood samples at 5000 rpm and 4 °C for 10 minutes. To precipitate the endogenous proteins in the plasma, a 50 μL aliquot of plasma sample was mixed with 200 μL of methanol containing acetic acid (2%, V/V) and 5 μL of a methanolic solution containing rutin (0.2 μg mL^{-1}, IS). The mixture was vortexed twice for two minutes with a 2 minute interval. After centrifugation at 12

000 rpm and 4 °C for 10 minutes, the supernatant was stored at −80 °C until analysis.

2.7. Identification of CGA metabolites in plasma by UPLC-QTOF-MS

The CGA metabolites in plasma were identified on an AB Sciex Q-TOF 5600-plus mass spectrometer (AB Sciex Corporation, Foster City, CA) coupled with a Shimadzu LC-30A liquid chromatograph (Shimadzu Corporation, Kyoto, Japan) in full-scan untargeted mode with a mass range of m/z 50–1000. Mobile phases consisting of ultrapure water (with 0.1% formic acid, solvent A) and acetonitrile (solvent B) were used to achieve chromatographic separation on an Agilent ZORBAX RRHD EclipsePlus C18 column (2.1 × 100 mm, 1.8 μm, Agilent Technology, Wilmington, DE, USA). The elution procedures were as follows: 0.01–15 min, 5–40% (B); 15–30 min, 40–95% (B); 30–32 min, 95% (B); 32–32.1 min, 95–5%. The experiment was conducted with a flow rate of 0.3 mL min^{-1}, an injection volume of 2 μL, and a column temperature of 40 °C. MS analysis was conducted in the negative ion mode with the following parameters: ion spray voltage of −4500 V, temperature of 500 °C, ion source gas1 at 40 psi, ion source gas2 at 50 psi, curtain gas at 40 psi, as well as declustering potential, collision energy, and collision energy spread at 100 V, −40 V, and 10 V, respectively. The metabolites were identified through their $[M–H]^{-1}$ and MS^2 spectra.

2.8. Quantitative determination of CGA and its metabolites by UPLC-QqQ-MS/MS

An UPLC-QqQ-MS/MS system consisting of a Shimadzu LC-30A liquid chromatograph and an AB Sciex 5500 triple quadrupole mass spectrometer (AB Sciex Corporation, Foster City, CA) was used to determine the concentrations of CGA and its metabolites in plasma. Ultrapure water (containing 0.1% formic acid, solvent A) and acetonitrile (solvent B) were used as mobile phases to achieve chromatographic separation on an Agilent ZORBAX RRHD EclipsePlus C_{18} column (2.1 × 100 mm, 1.8 μm, Agilent Technology, Wilmington, DE, USA). The elution procedures were as follows: 0–0.5 min, 5% (B); 0.5–2.5 min, 5–95% (B); 2.5–5 min, 95% (B); 5–5.1 min, 95–5% (B); 5.1–7 min, 5% (B). The flow rate was 0.3 mL min^{-1}, with an injection volume of 2 μL and a column temperature of 40 °C. MRM model was used and the MS parameters were set as follows: ion spray voltage of −4500 V, temperature of 500 °C, ion source gas1 at 40 psi, ion source gas2 at 50 psi, and curtain gas at 40 psi. The entrance potential (EP), collision cell exit potential (CXP), declustering potential (DP), and collision energy (CE) were operated at −10, −17, −60, and −25 V, respectively. The precursor-to-production transition of CGA was monitored at m/z 353 → 191.

The calibration curves were based on the concentration of CGA (5 to 30 μg mL^{-1}) in plasma as the X value and the peak area ratio (CGA/rutin) as the Y value. The linear regression equation was $Y = 70.488X - 0.1802$, with a correlation coefficient of 0.9992. To simulate the pharmacokinetic parameters, the non-compartmental statistical model in PKSolver V2.0 software was used.[21] The parameters measured in this study include the time taken to reach C_{max} (T_{max}), the area under the concentration–time curve (AUC), the mean residence time (MRT), the maximal plasma concentration (C_{max}), the elimination half-life ($t_{1/2}$), and the clearance (CL).

2.9. Statistical analysis

All data were expressed as means ± standard deviations (SD). SPSS 22.0 software was used for the analysis of the results of the orthogonal tests and one-way analysis of variance (ANOVA). And the differences were considered significant when $P < 0.05$. Origin 2019b software was used for drawing.

3. Results and discussion

3.1. Optimization of CGA-TPGS-LP formula

During the preparation of the thin film, lecithin is arranged in a bilayer membrane, which then forms a vesicle with an internal cavity. Chol is added to the middle of the bilayer to regulate fluidity. The hydrophobic portion of TPGS is immobilised in the membrane, while the hydrophilic portion is exposed outside the membrane surface. This results in better dispersion of liposomes and less aggregation in the aqueous solution.[22] On the other hand, the combination with TPGS effectively increases the cellular uptake of liposomal preparations by inhibiting the efflux pump ATPase and reduces the oxidative stress by scavenging free radicals.[23] Following the end of dialysis, a concentration gradient of Ca^{2+} was established due to the higher concentration of Ca^{2+} inside the vesicles compared to the outside. As a result, CGA was transported across the bimolecular membrane into the interior of the vesicle *via* ion drive.

In this experiment, the optimized concentration levels of four factors were selected as references for further $L_9(3)^4$ orthogonal matrix experiments to optimize the preparation conditions of liposomes based on the pre-experimental results.

As listed in Table 2, all the treatments had the positive effects on improving the EE. The indicator values depended on the variation of combined materials, and the experimental values of EE ranged from 61.54% to 82.60%. According to the R_j values, the influential sequence of various factors on EE was B (SPC/CGA) > C (SPC/Chol) > D (SPC/TPGS) > A (SPC). Comparative experiments were conducted between $A_2B_3C_2D_2$ and $A_2B_3C_2D_1$, as the former had the highest K_{ij} values and was not included in the orthogonal test, $A_2B_3C_2D_1$ was the best combination among all nine experimental groups. The combination of $A_2B_3C_2D_2$ with an EE of 83.22 ± 0.11% was chosen as the optimum materials formulation, and its LE was also excellent at 11.21 ± 0.02%. These results demonstrate the necessity of optimizing the materials formulations.

3.2. Particle size, polydispersity index (PDI) and zeta potential of liposomes

As shown in Fig. 1A and Table 3, the optimal formulation group of CGA-TPGS-LP had a particle size of 99.79 ± 0.49 nm, a PDI of 0.185 ± 0.011, and a zeta potential of −31.43 ± 0.84 mV. In comparison to CGA-LP, which had a particle size of 113.22 ± 1.10 nm, a PDI of 0.273 ± 0.020, and a zeta potential of −25.76 ±

Table 2 The orthogonal optimization test result

	Factors				
	A	B	C	D	
No.	SPC (mg)	SPC/CGA (w/w)	SPC/Chol (w/w)	SPC/TPGS (w/w)	The EE (%)
1	1	1	1	1	61.54
2	1	2	2	2	80.81
3	1	3	3	3	75.81
4	2	3	2	1	82.60
5	2	1	3	2	69.55
6	2	2	1	3	76.05
7	3	2	3	1	74.75
8	3	3	1	2	81.52
9	3	1	2	3	69.98
k_1	72.72	67.02	73.04	72.96	
k_2	76.07	77.20	77.79	77.29	
k_3	75.41	79.98	73.37	73.95	
R_j	3.35	12.95	4.76	4.33	
Best level	A_2	B_3	C_2	D_2	

1.59, CGA-TPGS-LP exhibited a smaller particle size and PDI value, as well as a higher absolute zeta potential value. The relatively small size of particles in CGA-TPGS-LP increases the likelihood of capture by the gastrointestinal tract when administered orally.[24] Additionally, the low PDI value indicates a relatively low variance in particle size. Furthermore, the

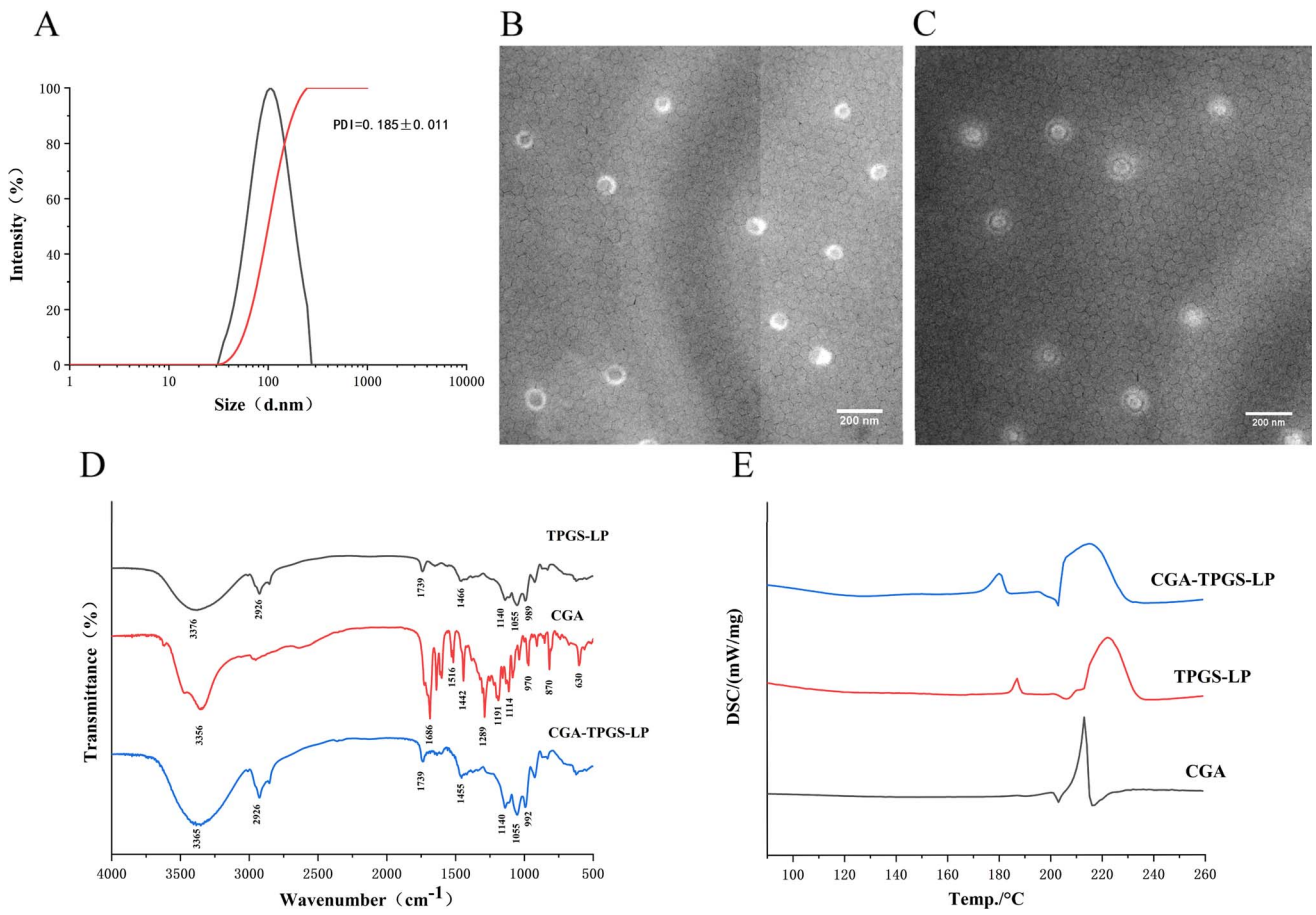

Fig. 1 (A) Particle size distribution of TPGS-coated liposomes; (B) TEM image of CGA-LP; (C) the enlarged TEM image of CGA-TPGS-LP; (D) FTIR spectra of TPGS-LP, CGA and CGA-TPGS-LP; (E) DSC profiles of TPGS-LP, CGA and CGA-TPGS-LP.

Table 3 Physical and chemical parameters of liposomes

	Particle size/nm	PDI	Zeta potential/mV
CGA-TPGS-LP	99.79 ± 0.85	0.185 ± 0.011	−31.43 ± 0.84
TPGS-LP	97.56 ± 0.22	0.176 ± 0.005	−33.23 ± 0.69
CGA-LP	113.22 ± 1.10	0.273 ± 0.020	−25.76 ± 1.59

surface charge of the liposome became more negative as a result of the formation of a densely packed TPGS hydrophilic layer on its surface. This layer helps to maintain the stability of the liposomes by reducing aggregation between them through electrostatic repulsion. Moreover, higher absolute values of zeta-potential prevent particle precipitation and protein adsorption during blood circulation.[25]

3.3. The drug content of CGA-LP and CGA-TPGS-LP

The LE of CGA-TPGS-LP and CGA-LP was found to be 11.21 ± 0.02% and 8.70 ± 0.23%, respectively. The EE of CGA-TPGS-LP and CGA-LP was found to be 83.22 ± 0.11% and 51.34 ± 0.32%, respectively. These results suggest that TPGS modification significantly improves the LE and EE of liposomes by 128.85% and 162.09%, respectively, compared to conventional liposomes. Moreover, during the HPLC measurement of the EE of liposomes, it was observed that CGA released from CGA-TPGS-LP exhibited a characteristic absorption peak at 327 nm, which was consistent with the absorption peak of free CGA.[26] This indicates that the chemical structure of CGA was preserved after being entrapped in the TPGS-modified liposomes.

3.4. Physicochemical characterization of CGA-TPGS-LP

The scanning transmission electron microscope (TEM) images of CGA-LP and CGA-TPGS-LP were presented in Fig. 1B and C, respectively. Spherical vesicle particles of uniform size were observed and evenly dispersed. The average size of these particles was approximately 100 nm, consistent with the findings from particle size analysis. Similar images can be found in the literature, where liposome samples were also observed using TEM after staining with phosphotungstic acid as the negative staining material.[27,28] The transmission electron microscopy (TEM) images confirmed the presence of a TPGS coating on the surface of the liposomes which was formed by its hydrophilic tail chain (refer to Fig. 1C). Similar results were obtained in the case of TPGS-modified PTX-liposomes.[29]

To demonstrate the interactions between the encapsulated drug and excipients, the formed samples underwent FTIR analysis. The infrared absorption spectra of CGA, TPGS-LP, and CGA-TPGS-LP were shown in Fig. 1D. The characteristic peaks at 2926 cm^{-1} (asymmetric stretching of CH_2 and CH_3) and 1466 cm^{-1} (symmetric stretching of CH_2 and CH_3) were from the hydrocarbon chain in the bilayer of liposomes.[30] Meanwhile, the stretching of O–H at 3438 cm^{-1}, which is considered a characteristic absorption peak of the liposomes, was shifted in the test sample to 3376 cm^{-1} for TPGS-LP and 3365 cm^{-1} for CGA-TPGS-LP. The asymmetric and symmetric stretching of PO^{2-} from the liposomes were represented by the characteristic peaks of TPGS-LP and CGA-TPGS-LP at 1140 cm^{-1} and 1055 cm^{-1}, respectively.[30] The peak at 1739 cm^{-1} in TPGS-LP and CGA-TPGS-LP is a characteristic of the C=O stretching resulting from the aliphatic ester bond between the hydrocarbon chain and phosphate group. This confirms the formation of a TPGS-modified lipid bilayer, as reported by Sonali, *et al.*[31] CGA exhibits multiple characteristic absorption peaks ranging from 500 cm^{-1} to 2000 cm^{-1}. However, many of the characteristic peaks of CGA were absent in CGA-TPGS-LP, such as 1191 cm^{-1} and 1516 cm^{-1},[32] confirming the encapsulation of the drug inside the liposomes.

Fig. 1E shows that CGA exhibited a clear endothermic peak at 213 °C, indicating its crystalline nature. In the DSC curves of TPGS-LP, the peak ranging from 215 to 230 °C was caused by the melting of TPGS-LP.[33] Meanwhile, the peak at 187 °C was formed by the lyophilized protective agent sucrose. However, in CGA-TPGS-LP, the crystal melting peak of CGA was not observed, while the peak of TPGS-LP and sucrose was retained. This result confirms that CGA was encapsulated in CGA-TPGS-LP in an amorphous form.

3.5. Stability during storage of CGA-TPGS-LP

The study compared the storage stability of CGA-TPGS-LP and CGA-LP over a 30 day period, with encapsulation rates measured at 5 day intervals. Table 4 shows that both formulations experienced a gradual decrease in encapsulation rate during storage. However, the rate of decrease for CGA-TPGS-LP (13.37%) was lower than that of CGA-LP (19.97%). By the 30th day, the encapsulation rate of CGA-TPGS-LP remained above 70%, while that of CGA-LP was only 30.46%. The storage stability of TPGS-modified liposomes is excellent because TPGS prevents liposome aggregation and rupture. Furthermore, the vitamin E component of TPGS offers antioxidant protection, which is a crucial factor in maintaining stability during liposome storage.[34]

3.6. *In vitro* release study of CGA from the liposome in SGF and SIF

The cumulative release percentages of drugs from carriers are considered as a crucial criterion for evaluating the effectiveness of oral drug applications. By prolonging the release time, the effects of active drugs can be enhanced.[35]

Table 4 The EE of CGA-TPGS-LP and CGA-LP at 4 °C for 30 days storage period

	EE (%)	
Day	CGA-TPGS-LP	CGA-LP
1	83.50 ± 2.20	50.43 ± 1.26
5	81.32 ± 1.52	47.05 ± 2.57
10	79.01 ± 3.48	42.04 ± 3.80
15	77.41 ± 3.13	38.64 ± 2.93
20	75.54 ± 1.66	34.46 ± 2.61
25	72.40 ± 5.31	32.06 ± 3.03
30	70.13 ± 4.62	30.46 ± 3.64

In vitro drug release experiments were performed to observe the drug release profiles of free CGA and CGA-TPGS-LP in simulated gastric and intestinal fluids. Fig. 2A shows that both free CGA and CGA-TPGS-LP exhibited rapid drug release within the initial 3 h, which subsequently slowed down, consistent with previous studies in simulated gastric juice.[36] However, the drug release rate of CGA-TPGS-LP was lower than that of free CGA, with release rates of 62.03% and 73.16% at the 3rd h, and 82.12% and 88.10% at the 12th hour, respectively. The fast drug release may be attributed to the destructive effect of the lower pH in simulated gastric fluid on the liposomes. Fig. 2B shows that during the 12 hour incubation period, CGA-TPGS-LP demonstrated a significant slow-release effect compared to free CGA. Furthermore, it was observed that the drug was released more slowly in alkaline intestinal fluids than in acidic environments. These results suggest that TPGS-modified liposomes can prolong drug release and improve drug bioutilization after oral administration.

3.7. Identification of CGA metabolites in plasma by UPLC-QTOF-MS

UPLC-QTOF-MS was used to identify the metabolites of CGA in rat plasma. The absorption and primary metabolism of polyphenols and flavonoids often occur in the intestinal epithelial cells. Further metabolism involves sulfation and/or glucuronidation, methylation, and hydrogenation in the liver.[37] The metabolites were then transported to body tissues through the circulatory system. In addition to CGA, ten metabolites were found in rat plasma after oral administration. The analysed metabolites included methylated CGA (CGA-Methyl), CGA glucuronide (CGA-Glu), caffeic acid (CA), CA glucuronide (CA-Glu), ferulic acid (FA), FA glucuronide (FA-Glu), FA sulfate (FA-Sul), dihydrocaffeic acid (DHCA), quinic acid (QA), and benzoic acid (BA). Fig. 3 and S1† illustrate the molecular ion and MS^2 fragment ion spectra of these metabolites. The CGA compound, with a molecular formula of $C_{16}H_{18}O_9$, exhibited $[M-H]^-$ at *m*/*z* 353.0848. Its main characteristic fragment ion was *m*/*z* 191, resulting from the loss of caffeic acid after breaking the ester bond between caffeic acid and quinic acid.[38] CGA-Methyl and CGA-Glu exhibited $[M-H]^-$ at *m*/*z* 367.1021 and 529.1205, respectively, which were 14 Da ($-CH_3$) and 176 Da (glucuronide) higher than deprotonated CGA.[39] Their other fragment ions were the same as those of CGA. The $[M-H]^-$ of CA was at *m*/*z* 179.0353. The main characteristic fragment ions of CA are *m*/*z* 135 and 134.[40] The fragment ion at *m*/*z* 135 results from the loss of a carboxyl group. While the fragment ion at *m*/*z* 134 is formed by the detachment of a hydrogen atom from the O–H group in the ion at *m*/*z* 135. The $[M-H]^-$ of CA-Glu is at *m*/*z* 355.0659, and its fragment ions, which lose glucuronic acid moieties, are the same as those of CA. DHCA, $[M-H]^-$ at *m*/*z* 181.0478, was produced by hydrogenating the double bonds in CA, resulting in a formula with two additional hydrogen atoms compared to CA. FA, a type of methylated compound of CA, exhibits $[M-H]^-$ at *m*/*z* 193.0463, which is 14 Da ($-CH_3$) higher than CA. Additionally, FA-Glu and FA-Sul have $[M-H]^-$ values of *m*/*z* 369.0824 and 273.0078, respectively. QA and BA were also detected, with $[M-H]^-$ values of *m*/*z* 191.0564 and 121.0296, respectively. It is worth noting that BA is formed after the metabolization of QA by intestinal microbiota due to the unstable structure of QA. In the study by Stalmach *et al.*,[41] twelve metabolites were identified in human plasma after coffee consumption. Their study found more sulphates, which differed from our results. This difference could be attributed to the presence of various isomerised CGA in coffee. Additionally, different intake may lead to different metabolites.

3.8. Bioavailability enhancement of CGA in liposomes

After oral administration of CGA and CGA-TPGS-LP suspension, the quantification of CGA and its major metabolites with concentrations above the limit of quantitation in rat plasma was performed by UPLC-QqQ-MS/MS.

According to the results of UPLC-QTOF-MS, the ion pairs used for the MRM analysis of these analytes were *m*/*z* 353.0804/191.0851 (CGA), 367.0992/191.0647 (CGA-methyl), 355.0592/

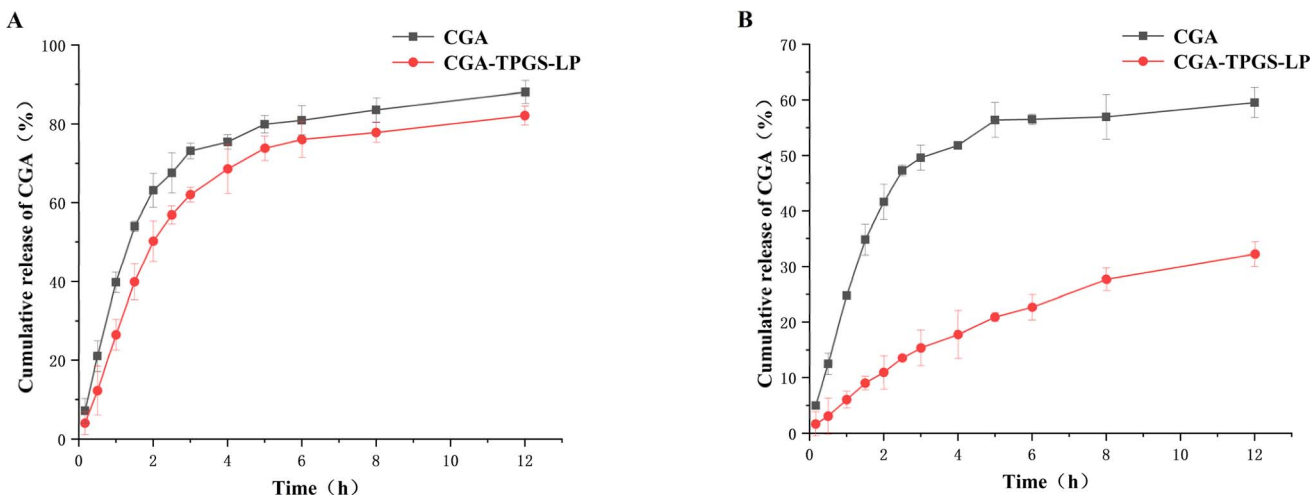

Fig. 2 Release of CGA solution and CGA-TPGS-LP in simulated gastric fluid (A) and simulated intestinal fluids (B).

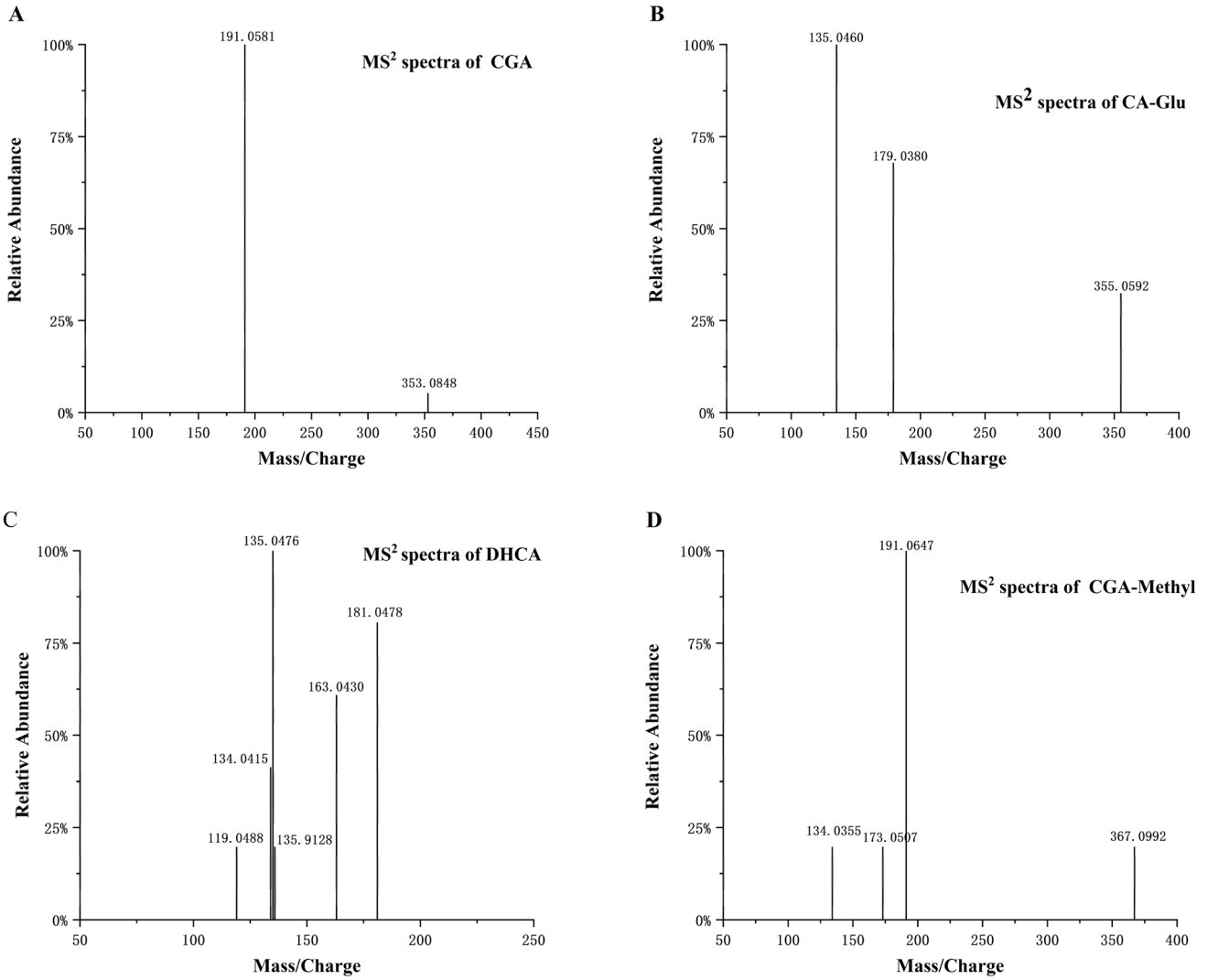

Fig. 3 The MS^2 spectra of CGA (A), CA-Glu (B), DHCA (C) and CGA-Methyl (D) in plasma obtained by UPLC-QTOF-MS.

135.0460 (CA-Glu) and 181.0478/135.0476 (DHCA), respectively. Rutin with an ion pair of *m/z* 609/300 was selected as internal standard (IS). The CGA concentration in rat plasma was calculated from the peak area ratio (CGA/IS) according to the calibration curve. For three metabolites, changes in concentration were reflected by changes in peak area ratios, as no authentic standard was available.

Fig. 4A illustrates the plasma concentration–time profile of CGA and its main metabolites after oral administration. The pharmacokinetic parameters were calculated using PKSolver V2.0 software and were presented in Table 5.

Following oral administration, the plasma concentration of CGA increased rapidly in both groups, reaching its maximum concentration at 0.5 h. This increase may be attributed to the absorption of partial polyphenols in the stomach through monocarboxylic acid transporter-mediated transport systems,[42] dihydromyricetin[43] and quercetin[39] also showed a rapid increase in plasma drug concentrations after intragastric administration in rats. CGA-TPGS-LP and CGA groups exhibited similar maximum plasma concentrations (C_{max}) of 100.75 ± 10.3 ng mL^{-1} and 110.44 ± 9.2 ng mL^{-1}, respectively. The absorption of free polyphenols occurs mainly through passive diffusion, and water-soluble CGA has an advantage in terms of diffusion. The encapsulation of liposomes did not affect the concentration gradient of CGA during passive diffusion, as indicated by the approximate maximum blood concentration. The drug elimination half-life ($t_{1/2}$) was prolonged from 1.58 ± 0.23 h to 2.53 ± 0.7 h after oral administration of CGA-TPGS-LP compared to free CGA. The mean residence time (MRT) (0–∞) was also prolonged from 2.47 ± 0.12 h to 3.77 ± 0.22 h. The AUC (0–∞) of CGA-TPGS-LP (423.87 ± 34.6 ng h mL^{-1}) was enhanced about 1.52-fold compared with free CGA (284.51 ± 26.4 ng h mL^{-1}).

Similar improvement effects were also observed in CGA metabolites (Fig. 4B–D). The plasma concentrations of DHCA, CA-Glu and CGA-Methyl increased rapidly in line with CGA within 0.5 or 1 h after oral administration, and their maximum plasma concentrations in the CGA-TPGS-LP group were higher than those in the CGA group. The metabolites showed a slower

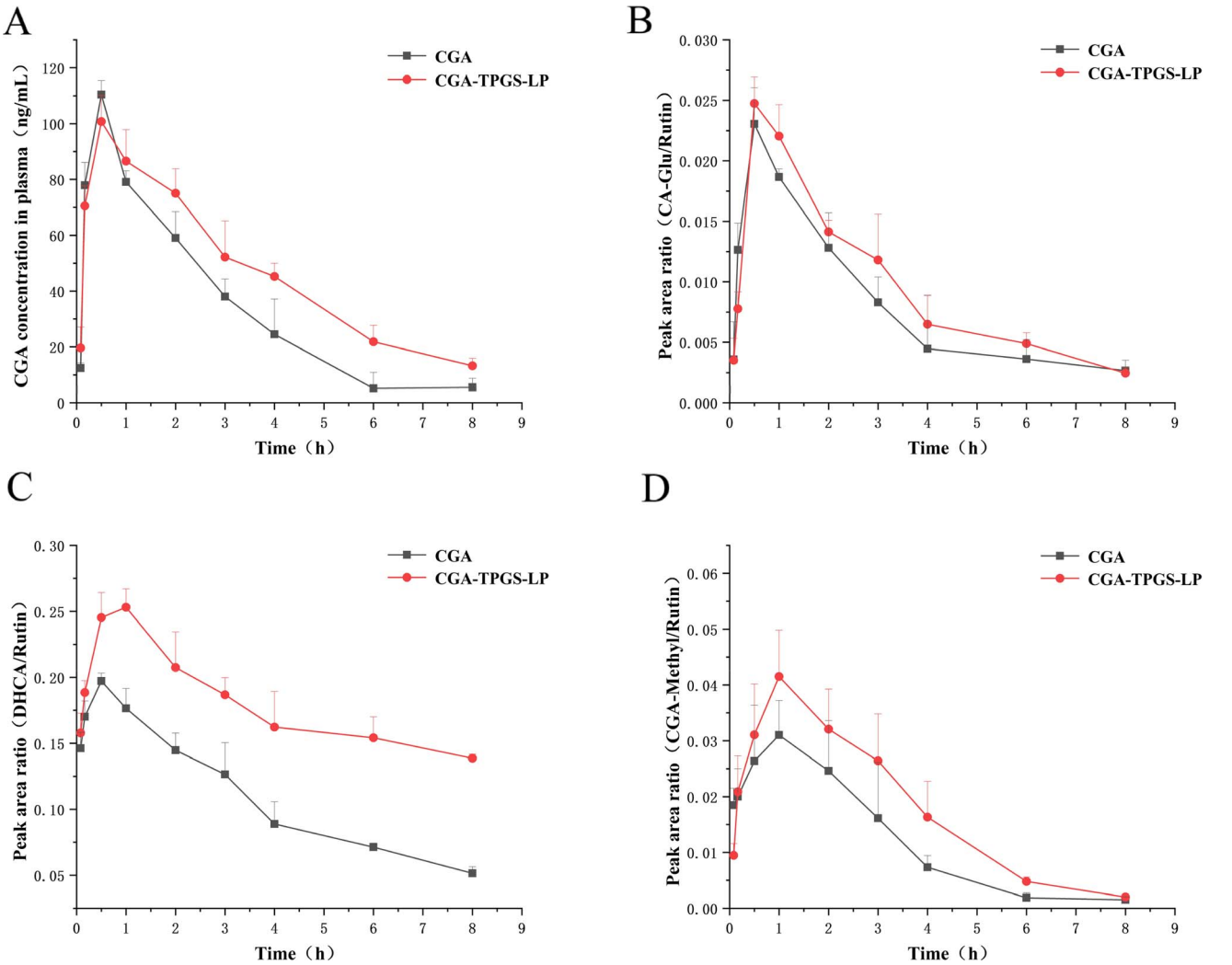

Fig. 4 Temporal profiles of CGA and its metabolite concentrations in plasma of rats in the CGA group and CGA-TPGS-LP group. (A) CGA; (B) CA-Glu; (C) DHCA; (D) CGA-Methyl.

Table 5 Pharmacokinetic parameters of rats in the CGA group and CGA-TPGS-LP group

Parameters	CGA	CGA-TPGS-LP
C_{max} (ng mL^{-1})	110.44 ± 9.2	100.75 ± 10.3
$AUC_{(0-t)}$ (ng h mL^{-1})	271.68 ± 22.9	375.33 ± 30.5
$AUC_{(0-\infty)}$ (ng h mL^{-1})	284.51 ± 26.4	423.87 ± 34.6
T_{max} (h)	0.5 ± 0	0.5 ± 0
$t_{1/2}$ (h)	1.58 ± 0.23	2.53 ± 0.7
CL ((mg) (ng^{-1} mL^{-1}) h^{-1})	0.14 ± 0.02	0.09 ± 0.02
$MRT_{(0-\infty)}$ (h)	2.47 ± 0.12	3.77 ± 0.22

rate of decline in the CGA-TPGS-LP group compared to the CGA group after reaching maximum plasma concentrations. The results indicate a slow-release effect of drugs encapsulated in TPGS-modified liposomes.

Some of the metabolites present advantages in improving human health, for instance, DHCA can alleviate adverse effects on emotion of rat that long-term exposure to low-dose Polystyrene nano-plastics *via* the cAMP/PKA/p-CREB/Atp2b2 signaling pathway.[44] Therefore, it is important to consider the influence of the vehicle on the metabolites of the carried drug in future studies.

4. Conclusion

The CGA-TPGS-LP was prepared using the thin film dispersion method in combination with the ion gradient technique. The optimized formula consisted of 400 mg of SPC and a mass ratio of SPC to CGA, Chol, TPGS at 5 : 1, 7 : 1, and 8 : 1, respectively. TPGS-LP containing CGA was successfully produced with an entrapment efficiency of 83.22 ± 0.11% and a drug loading efficiency of 11.21 ± 0.02% following formulation optimization. The CGA-TPGS-LP was a spherical nanoparticle with a diameter of 99.79 ± 0.49 nm, a PDI of 0.185 ± 0.011, and a zeta potential of −31.43 ± 0.84 mV. The TEM, FTIR, and DSC characterization results confirmed that liposome membrane were composed of lecithin, cholesterol, and TPGS lipophilic head with a TPGS

hydrophilic tail chain coating on its surface and CGA was encapsulated in an amorphous form within the TPGS-modified liposomes. The TPGS-modified liposomes exhibited higher entrapment efficiency and better storage stability. The *in vivo* test results demonstrated a 1.52-fold increase in the bioavailability of CGA in TPGS-LP in rats. Additionally, the three main metabolites of CGA had higher plasma concentrations and slower degradation rate.

Data availability

The data supporting this article have been included as part of the ESI.†

Conflicts of interest

There are no conflicts to declare.

Acknowledgements

This study was financially supported by the National Natural Science Foundation of China (Grant No. 32060535), and the Modern Agricultural Research System of Jiangxi Province (Grant No. JXARS-03).

References

1 D. Y. Wang, X. M. Zhao and Y. L. Liu, Hypoglycemic and hypolipidemic effects of a polysaccharide from flower buds of Lonicera japonica in streptozotocin-induced diabetic rats, *Int. J. Biol. Macromol.*, 2017, **102**, 396–404, DOI: 10.1016/j.ijbiomac.2017.04.056.

2 X. T. Chen, T. Yu, Q. S. Kong, H. Xu, Z. Y. Zhao, G. C. Li, H. J. Fan and Y. B. Wang, A chlorogenic acid functional strategy of anti-inflammation, anti-coagulation and promoted endothelial proliferation for bioprosthetic artificial heart valves, *J. Mater. Chem. B*, 2023, **B11**(12), 2663–2673, DOI: 10.1039/d2tb02407a.

3 J. h. Xiong, S. C. Li, W. J. Wang, Y. P. Hong, K. J. Tang and Q. S. Luo, Screening and identification of the antibacterial bioactive compounds from Lonicera japonica Thunb. leaves, *Food Chem.*, 2013, **138**(1), 327–333, DOI: 10.1016/j.foodchem.2012.10.127.

4 J. Tošović, S. Marković, J. M. Dimitrić Marković, M. Mojović and D. Milenković, Antioxidative mechanisms in chlorogenic acid, *Food Chem.*, 2017, **237**, 390–398, DOI: 10.1016/j.foodchem.2017.05.080.

5 G. J. Shang, S. Y. Liu, R. Zhu, D. L. Li, S. T. Meng, Y. T. Wang and L. F. Wu, Chlorogenic acid improves common carp (Cyprinus carpio) liver and intestinal health through Keap-1/Nrf2 and NF-κB signaling pathways: Growth performance, immune response and antioxidant capacity, *Fish Shellfish Immunol.*, 2024, **146**, 109378, DOI: 10.1016/j.fsi.2024.109378.

6 K. Cheng, J. Y. Niu, J. Y. Zhang, Y. N. Qiao, G. R. Dong, R. Guo, X. T. Zheng, Z. H. Song, J. Huang, J. R. Wang and Y. Zhang, Hepatoprotective effects of chlorogenic acid on mice exposed to aflatoxin B1: Modulation of oxidative stress and inflammation, *Toxicon*, 2023, **231**, 107177, DOI: 10.1016/j.toxicon.2023.107177.

7 W. L. Liu, Y. Y. Hou, Y. Y. Jin, Y. P. Wang, X. K. Xu and J. Z. Han, Research progress on liposomes: Application in food, digestion behavior and absorption mechanism, *Trends Food Sci. Technol.*, 2020, **104**, 177–189, DOI: 10.1016/j.tifs.2020.08.012.

8 K. Singpanna, K. Dechsri, P. Patrojanasophon, P. Limpachayaporn, P. Opanasopit and N. Nuntharatanapong, Transdermal delivery, cytotoxicity and anti-melanogenic activity of p- chlorophenyl benzyl ether loaded-liposomes, *J. Drug Delivery Sci. Technol.*, 2021, **65**, 102746, DOI: 10.1016/j.jddst.2021.102746.

9 X. L. Zhang, Q. L. Qu, A. Y. Zhou, Y. L. Wang, J. Zhang, R. H. Xiong, V. Lenders, B. B. Manshian, D. W. Hua, S. J. Soenen and C. B. Huang, Core-shell microparticles: From rational engineering to diverse applications, *Adv. Colloid Interface Sci.*, 2022, **299**, 102568, DOI: 10.1016/j.cis.2021.102568.

10 Y. X. Cai, Y. Y. Zhang, Q. L. Qu, R. H. Xiong, H. Tang and C. B. Huang, Encapsulated Microstructures of Beneficial Functional Lipids and Their Applications in Foods and Biomedicines, *J. Agric. Food Chem.*, 2022, **70**(27), 8165–8187, DOI: 10.1021/acs.jafc.2c02248.

11 N. Dhiman, J. Sarvaiya and P. Mohindroo, A drift on liposomes to proliposomes: recent advances and promising approaches, *J. Liposome Res.*, 2022, **32**(4), 317–331, DOI: 10.1080/08982104.2021.2019762.

12 C. L. Yang, T. T. Wu, Y. Qi and Z. P. Zhang, Recent Advances in the Application of Vitamin E TPGS for Drug Delivery, *Theranostics*, 2018, **8**(2), 464–485, DOI: 10.7150/thno.22711.

13 D. S. Kim, D. W. Kim, K. S. Kim, J. S. Choi, Y. G. Seo, Y. S. Youn, K. T. Oh, C. S. Yong, J. O. Kim, S. G. Jin and H.-G. Choi, Development of a novel l-sulpiride-loaded quaternary microcapsule: Effect of TPGS as an absorption enhancer on physicochemical characterization and oral bioavailability, *Colloids Surf., B*, 2016, **147**, 250–257, DOI: 10.1016/j.colsurfb.2016.08.010.

14 H. J. Lu, Z. M. Tian, Y. Y. Cui, Z. C. Liu and X. Y. Ma, Chlorogenic acid: A comprehensive review of the dietary sources, processing effects, bioavailability, beneficial properties, mechanisms of action, and future directions, *Compr. Rev. Food Sci. Food Saf.*, 2020, **19**(6), 3130–3158, DOI: 10.1111/1541-4337.12620.

15 Z. Q. Ge, X. Y. Du, X. N. Huang and B. Qiao, Enhanced oral bioavailability of ursolic acid nanoparticles via antisolvent precipitation with TPGS1000 as a stabilizer, *J. Drug Delivery Sci. Technol.*, 2015, **29**, 210–217, DOI: 10.1016/j.jddst.2015.08.001.

16 M. A. Farooq, X. Y. Huang, A. Jabeen, A. Ahsan, T. A. Seidu, P. T. Kutoka and B. Wang, Enhanced cellular uptake and cytotoxicity of vorinostat through encapsulation in TPGS-modified liposomes, *Colloids Surf., B*, 2021, **199**, 111523, DOI: 10.1016/j.colsurfb.2020.111523.

17 D. A. Fernandes, Liposomes for Cancer Theranostics, *Pharmaceutics*, 2023, **15**(10), 2448, DOI: 10.3390/pharmaceutics15102448.
18 Q. S. Jin, H. L. Li, Z. H. Jin, L. J. Huang, F. Z. Wang, Y. Zhou, Y. M. Liu, C. L. Jiang, J. Oswald, J. H. Wu and X. R. Song, TPGS modified nanoliposomes as an effective ocular delivery system to treat glaucoma, *Int. J. Pharm.*, 2018, **553**(1–2), 21–28, DOI: 10.1016/j.ijpharm.2018.10.033.
19 L. D. Du, D. M. Li, J. J. Zhang, J. Du, Q. S. Luo and J. H. Xiong, Elicitation of Lonicera japonica Thunb suspension cell for enhancement of secondary metabolites and antioxidant activity, *Ind. Crops Prod.*, 2020, **156**, 112877, DOI: 10.1016/j.indcrop.2020.112877.
20 D. Zheng and Q. F. Zhang, Bioavailability Enhancement of Astilbin in Rats through Zein–Caseinate Nanoparticles, *J. Agric. Food Chem.*, 2019, **67**(20), 5746–5753, DOI: 10.1021/acs.jafc.9b00018.
21 Y. Zhang, M. R. Huo, J. P. Zhou and S. F. Xie, PKSolver: An add-in program for pharmacokinetic and pharmacodynamic data analysis in Microsoft Excel, *Comput. Methods Progr. Biomed.*, 2010, **99**(3), 306–314, DOI: 10.1016/j.cmpb.2010.01.007.
22 C. Caddeo, L. Pucci, M. Gabriele, C. Carbone, X. Fernàndez-Busquets, D. Valenti, R. Pons, A. Vassallo, A. M. Fadda and M. Manconi, Stability, biocompatibility and antioxidant activity of PEG-modified liposomes containing resveratrol, *Int. J. Pharm.*, 2018, **538**(1–2), 40–47, DOI: 10.1016/j.ijpharm.2017.12.047.
23 E. M. Collnot, C. Baldes, M. F. Wempe, R. Kappl, J. Hüttermann, J. A. Hyatt, K. J. Edgar, U. F. Schaefer and C. M. Lehr, Mechanism of inhibition of P-glycoprotein mediated efflux by vitamin E TPGS: Influence on ATPase activity and membrane fluidity, *Mol. Pharmaceutics*, 2007, **4**(3), 465–474, DOI: 10.1021/mp060121r.
24 Y. Shao, L. Han and H. K. Yang, TPGS-chitosome as an effective oral delivery system for improving the bioavailability of Coenzyme Q10, *Eur. J. Pharm. Biopharm.*, 2015, **89**, 339–346, DOI: 10.1016/j.ejpb.2014.12.026.
25 A. Nagayasu, K. Uchiyama and H. Kiwada, The size of liposomes: a factor which affects their targeting efficiency to tumors and therapeutic activity of liposomal antitumor drugs, *Adv. Drug Delivery Rev.*, 1999, **40**(1–2), 75–87, DOI: 10.1016/s0169-409x(99)00041-1.
26 T. Song, H. Wang, Y. Liu, R. Cai, D. Yang and Y. Xiong, TPGS-Modified Long-Circulating Liposomes Loading Ziyuglycoside I for Enhanced Therapy of Myelosuppression, *Int. J. Nanomed.*, 2021, **16**, 6281–6295, DOI: 10.2147/ijn.s326629.
27 X. J. Wang, L. Liu, S. Q. Xia, B. Muhoza, J. B. Cai, X. M. Zhang, E. Duhoranimana and J. K. Su, Sodium carboxymethyl cellulose modulates the stability of cinnamaldehyde-loaded liposomes at high ionic strength, *Food Hydrocolloids*, 2019, **93**, 10–18, DOI: 10.1016/j.foodhyd.2019.02.004.
28 S. J. Ma, R. Yu, Y. P. Mai, N. Yu, T. Gao and J. H. Yang, Enhanced Influenza Immunity by Nasal Mucosal Administration of the TPGS-Modified Liposomal Vaccine, *AAPS PharmSciTech*, 2022, **23**(7), 272, DOI: 10.1208/s12249-022-02425-3.
29 S. M. Han, J. S. Baek, M. S. Kim, S. J. Hwang and C.-W. Cho, Surface modification of paclitaxel- loaded liposomes using d-α-tocopheryl polyethylene glycol 1000 succinate: Enhanced cellular uptake and cytotoxicity in multidrug resistant breast cancer cells, *Chem. Phys. Lipids*, 2018, **213**, 39–47, DOI: 10.1016/j.chemphyslip.2018.03.005.
30 M. X. Xue, J. Wang and M. G. Huang, Inulin-Modified Liposomes as a Novel Delivery System for Cinnamaldehyde, *Foods*, 2022, **11**, 1467, DOI: 10.3390/foods11101467.
31 S. Sonali, P. Agrawal, R. P. Singh, C. V. Rajesh, S. Singh, M. R. Vijayakumar, B. L. Pandey and M. S. Muthu, Transferrin receptor-targeted vitamin E TPGS micelles for brain cancer therapy: preparation, characterization and brain distribution in rats, *Drug Delivery*, 2016, **23**(5), 1788–1798, DOI: 10.3109/10717544.2015.1094681.
32 D. Pujol, C. Liu, J. Gominho, M. À. Olivella, N. Fiol, I. Villaescusa and H. Pereira, The chemical composition of exhausted coffee waste, *Ind. Crops Prod.*, 2013, **50**, 423–429, DOI: 10.1016/j.indcrop.2013.07.056.
33 L. D. Liang, W. W. Cao, L. L. Li, W. C. Liu, X. Y. Wei, J. L. Chen, G. Y. Ren, Y. K. Zhao and X. Duan, Fabrication and characterisation of pea protein isolate-chlorogenic acid nanoparticles, *Int. J. Food Sci. Technol.*, 2024, **59**, 1615–1623, DOI: 10.1111/ijfs.16911.
34 A. R. Shah and R. Banerjee, Effect of D-alpha-tocopheryl polyethylene glycol 1000 succinate (TPGS) on surfactant monolayers, *Colloids Surf., B*, 2011, **85**(2), 116–124, DOI: 10.1016/j.colsurfb.2011.01.021.
35 K. Tahara, H. Tomida, Y. Ito, S. Tachikawa, R. Onodera, H. Tanaka, Y. Tozuka and H. Takeuchi, Pulmonary liposomal formulations encapsulated procaterol hydrochloride by a remote loading method achieve sustained release and extended pharmacological effects, *Int. J. Pharm.*, 2016, **505**(1–2), 139–146, DOI: 10.1016/j.ijpharm.2016.03.031.
36 A. Singh, A. Mhaske and R. Shukla, Fabrication of TPGS-Grafted Polyamidoamine Dendrimer for Enhanced Piperine Brain Delivery and Pharmacokinetics, *AAPS PharmSciTech*, 2022, **23**, 236, DOI: 10.1208/s12249-022-02393-8.
37 G. Williamson, C. D. Kay and A. Crozier, The Bioavailability, Transport, and Bioactivity of Dietary Flavonoids: A Review from a Historical Perspective, *Compr. Rev. Food Sci. Food Saf.*, 2018, **17**(5), 1054–1112, DOI: 10.1111/1541-4337.12351.
38 J. B Yang, L. W. Yao, K. Y. Gong, K. L. Li, L. Sun and W. Cai, Identification and Quantification of Chlorogenic Acids from the Root Bark of Acanthopanax gracilistylus by UHPLC-Q-Exactive Orbitrap Mass Spectrometry, *ACS Omega*, 2022, **7**, 25675–25685, DOI: 10.1021/acsomega.2c02899.
39 C. X. Sun, Y. Wei, R. R. Li, L. Dai and Y. X. Gao, Quercetagetin-Loaded Zein-Propylene Glycol Alginate Ternary Composite Particles Induced by Calcium Ions: Structure Characterization and Formation Mechanism, *J.*

Agric. Food Chem., 2017, **65**(19), 3934–3945, DOI: **10.1021/acs.jafc.7b00921**.

40 J. Q. Yuan, Y. T. Wang, S. Q. Mi, J. Y. Zhang and Y. X. Sun, Rapid screening and characterization of caffeic acid metabolites in rats by UHPLC-Q-TOF mass spectrometry, *Trop. J. Pharm. Res.*, 2021, **20**(2), 389–401, DOI: **10.4314/tjpr.v20i2.25**.

41 A. Stalmach, G. Williamson and A. Crozier, Impact of dose on the bioavailability of coffee chlorogenic acids in humans, *Food Funct.*, 2014, **5**(8), 1727–1737, DOI: **10.1039/c4fo00316k**.

42 Y. Konishi, Z. H. Zhao and M. Shimizu, Phenolic Acids Are Absorbed from the Rat Stomach with Different Absorption Rates, *J. Agric. Food Chem.*, 2006, **54**(20), 7539–7543, DOI: **10.1021/jf061554+**.

43 J. F. Zhou, G. D. Zheng, W. J. Wang, Z. P. Yin, J. G. Chen, J. E. Li and Q. F. Zhang, Physicochemical properties and bioavailability comparison of two quercetin loading zein nanoparticles with outer shell of caseinate and chitosan, *Food Hydrocolloids*, 2021, **120**, 106959, DOI: **10.1016/j.foodhyd.2021.106959**.

44 W. B. Jiang, C. Hu, Y. Y. Chen, Y. Li, X. Y. Sun, H. Y. Wu, R. M. Yang, Y. W. Tang, F. R. Niu, W. Wei, C. H. Sun and T. S. Han, Dysregulation of the microbiota-brain axis during long-term exposure to polystyrene nanoplastics in rats and the protective role of dihydrocaffeic acid, *Sci. Total Environ.*, 2023, **874**, 162101, DOI: **10.1016/j.scitotenv.2023.162101**.